ASM Sc. J., 12, Special Issue 1, 2019 for IQRAC2018, 60-70

A Stability Analysis of Solutions on Boundary Layer Flow Past a Moving Thin Needle in a Nanofluid with Slip Effect

Siti Nur Alwani Salleh*[1], Norfifah Bachok[1,2], Norihan Md Arifin[1,2], and Fadzilah Md Ali[1,2]

[1]*Institute for Mathematical Research, Universiti Putra Malaysia, 43400 UPM Serdang, Selangor, Malaysia*
[2]*Department of Mathematics, Faculty of Science, Universiti Putra Malaysia, 43400 UPM Serdang, Selangor, Malaysia*

**Corresponding author: alwani24salleh@gmail.com*

The purpose of this work is to study the effects of partial slip on the boundary layer flow over a moving horizontal thin needle in nanofluid. Three types of nanoparticles, namely, alumina, copper and titania are considered. The self-similar ordinary differential equations are obtained by adopting the similarity transformations and these equations are then solved numerically using bvp4c function in MATLAB software. Special emphasis has been given to the parameters of interest which include the nanoparticle volume fraction, slip, needle size and velocity ratio. The effect of these parameters on the velocity and temperature profiles, skin friction coefficient and heat transfer rate are further discussed through graphs. It is revealed from the study that the dual solutions exist when the needle oppose the direction of the fluid motion $\varepsilon < 0$, and the range of the possible solutions obtained is strongly depending on the needle size and slip parameters. The stability of the solutions is determined using a stability analysis. This analysis indicated that the upper branch solution is linearly stable and there is an initial decay of disturbance in the system. Meanwhile, the result is invertible for the lower branch solution.

Keywords: dual solutions, nanofluid, slip, stability analysis, thin needle.

I. Introduction

A few decade ago, fluid heating and cooling are most important subject in view of its applications in industries and engineering purposes. Such applications are power generation, manufacturing and also transportations. Generally, conventional fluids used in these applications such as kerosene, water, ethylene glycol and engine oil cannot meet the requirement of the cooling process. Experimentally, Choi (1995) introduced a new mixture between solid particles whose diameter is less than 100nm, called nanoparticles and the base fluid. This mixture is known as a nanofluid and has a tendency to improve the thermal conductivity of the conventional fluids drastically as needed by the industries. Interestingly, nanofluid possess some special characteristics where it is very stable and do not have any additional problem such as erosion, sedimentation, non-Newtonian behavior or additional pressure drop. This is due to the tiny size of nanoparticles and low volume fraction of nanoelements needed for the thermal conductivity improvement.

There are two models of nanofluid which familiar in fluid mechanics. First is the model proposed by Buongiorno (2006), and the second is the model proposed by Tiwari and Das (2007). Tiwari and Das model is a single phase model, where the nanoparticles and base fluid are said to be in thermal equilibrium, flowing at

a constant velocity and there is no-slip condition occurs between them. This model considers the influence of nanoparticles volume fraction. Different with the Tiwari and Das model, Buongiono's model is a two phase model, by which the slip velocity between nanoparticles and base fluid are not equal to zero. This model incorporates the effect of the Brownian motion and thermophoresis. There are some articles regarding these two models which can be found in the existing literature (Bachok et al., 2012,, Othman et al., 2017, Pandey and Kumar, 2017). Furthermore, nanofluid has many practical applications, especially in automotive applications, electronic devices and biomedical industries (Huminic and Huminic, 2012, Saidur et al., 2011, Wong and Leon, 2010).

The study of the boundary layer flow past a thin needle in a viscous fluid was first studied by Lee (1967). The needle is described as a parabolic of revolution with the axis in the direction of the incident flow. Moreover, the needle is considered "thin" when its thicknesses are smaller or comparable to that of the boundary layer on it. Some applications of the thin needle are coating of wires, hot wire anemometer for measuring the wind's velocity, the blood flow problem, lubrication as well as geothermal power generation. A few years later, Narain and Uberoi (1972, 1973) and Wang (1990) extended the Lee (1967) work by considering forced and mixed convection flow over a thin needle, respectively. Apart from that, the numerous works regarding the boundary layer behavior past a thin needle were carried out by some authors (Afridi and Qasim, 2018, Ahmad et al., 2008, Ishak et al., 2007). The consideration of the boundary layer flow over a thin needle immersed in nanofluid has been studied by Grosan and Pop (2011). They reported the classical problem of forced convection flow and heat transfer with a variable surface temperature. Then after, few researchers (Hayat et al., 2016, Krishna et al., 2017, Soid et al., 2017, Trimbitas et al., 2014) further the research in many aspects of the problem.

In all the above mentioned works, the authors focused their analysis on the boundary layer flow and heat transfer with no-slip boundary condition. Nevertheless, no-slip assumption does no longer consistent in certain flow situations and it must be replaced by a partial slip boundary condition (Bhattacharyya et al., 2012). The study about the slip effect was introduced by Beavers and Joseph (1967) considering a permeable wall in viscous fluid. The slip flows under different flow configurations have been studied by many researchers in recent years (Awais et al., 2016, Das, 2012, Uddin et al., 2018, Wang, 2002). However, no study has been performed to investigate the effect of the partial slip over a thin needle. Therefore, the aim of the present work is to analyze the effects of partial slip on the boundary layer flow over a moving thin needle in nanofluid with a stability analysis. Recently, stability analysis has attracted a lot of researches (Mahapatra and Nandy, 2011, Sharma et al., 2014, Yasin et al., 2017) due to the stable solutions offer a good physical meaning in the system. The nonlinear ordinary differential equations are solved numerically using bvp4c package in MATLAB and the results are discussed from the physical point of view in the next section.

II. Methodology

Consider two-dimensional laminar boundary layer flow and heat transfer on a moving horizontal thin needle in a nanofluid at a constant ambient temperature T_∞. The curved surface of the needle is kept at constant temperature T_w such that $T_w > T_\infty$. x and r represent the axial and radial coordinates in cylindrical form, respectively, where $r = R(x)$ is the radius of the needle. The needle moves with a constant velocity U_w in the same or opposite direction to the fluid flow of a constant velocity U_∞. Under these assumptions, the basic equations for the flow and heat transfer are given as

$$\frac{\partial}{\partial x}(ru) + \frac{\partial}{\partial r}(rv) = 0, \tag{1}$$

$$\frac{\partial u}{\partial t}+u\frac{\partial u}{\partial x}+v\frac{\partial u}{\partial r}=\frac{\mu_{nf}}{\rho_{nf}}\frac{1}{r}\frac{\partial}{\partial r}\left(r\frac{\partial u}{\partial r}\right), \quad (2)$$

$$\frac{\partial T}{\partial t}+u\frac{\partial T}{\partial x}+v\frac{\partial T}{\partial r}=\frac{\alpha_{nf}}{r}\frac{\partial}{\partial r}\left(r\frac{\partial T}{\partial r}\right). \quad (3)$$

We assume the initial and boundary conditions are as follows:

$$t<0: u(x,r,t)=v(x,r,t)=0,\ T(x,r,t)=T_\infty,$$

$$\begin{gathered} t\geq 0: u(x,r,t)=U_w+L\frac{\partial u}{\partial r},\ \ v(x,r,t)=0,\\ T(x,r,t)=T_w \ \text{ at } \ r=R(x),\\ u(x,r,t)\to U_\infty,\ \ T(x,r,t)\to T_\infty \ \text{ as } \ r\to\infty. \end{gathered} \quad (4)$$

in which u and v are the velocity components in the direction of x and r axis, respectively, T is the temperature of the fluid, L is the slip length, μ is the viscosity, α is the thermal diffusivity and ρ is the density in which the subscripts 's', 'f' and 'nf' represent 'solid', 'fluid' and 'nanofluid', respectively. According to Oztop and Abu-Nada (2008), the equations that relate these parameters are given by:

$$\begin{gathered} \rho_{nf}=(1-\phi)\,\rho_f+\phi\rho_s,\\ (\rho C_p)_{nf}=(1-\phi)\,(\rho C_p)_f+\phi\,(\rho C_p)_s\,,\\ \alpha_{nf}=\frac{k_{nf}}{(\rho C_p)_{nf}},\ \ \mu_{nf}=\frac{\mu_f}{(1-\phi)^{2.5}},\\ \frac{k_{nf}}{k_f}=\frac{(k_s+2k_f)-2\phi(k_f-k_s)}{(k_s+2k_f)+\phi(k_f-k_s)}, \end{gathered} \quad (5)$$

where the thermal conductivity, heat capacity and nanoparticle volume fraction for the nanofluid are given by k, (ρC_p) and ϕ, respectively.

Since this study considers the steady-state flow, we assume $\partial u/\partial t=0$ and $\partial T/\partial t=0$. Thus, the following similarity transformations have been introduced to solve the Equations (1)–(3) along with the boundary conditions (4):

$$\psi=\nu x f(\eta),\ \ \eta=\frac{Ur^2}{\nu x},\ \ \theta(\eta)=\frac{T-T_\infty}{T_w-T_\infty}. \quad (6)$$

Here $U=U_w+U_\infty$ is the composite velocity between the needle and the free stream flow, and ψ is the stream function which is defined as $u=r^{-1}\partial\psi/\partial r$ and $v=-r^{-1}\partial\psi/\partial x$. Noteworthy, the similarity transformations are a good mathematical simplification in order to reduce PDEs to ODEs. The reason why need to use the similarity transformations are that the PDEs have many independent variables x and r which are difficult to solve. Hence, the equations must reduce to ODEs with η as a new independent variable.

Setting $\eta=c$ which refer to the needle wall, Equation (6) prescribes the size and shape of the needle where its surface is given by:

$$R(x)=\left(\frac{\nu c x}{U}\right)^{1/2}. \quad (7)$$

Next, we obtain the following ordinary differential equations by substituting Equations (5) and (6) into the basic Equations (2)–(4):

$$\frac{2\eta}{A_1}f'''+\frac{2}{A_1}f''+ff''=0, \quad (8)$$

$$\frac{2\eta}{Pr}\frac{A_2}{A_3}\theta''+\frac{2}{Pr}\frac{A_2}{A_3}\theta'+f\theta'=0, \quad (9)$$

where

$$\begin{gathered} A_1=(1-\phi)^{2.5}\left[1-\phi+\phi\,(\rho_s/\rho_f)\right]\\ A_2=k_{nf}/k_f\\ A_3=1-\phi+\phi\,(\rho C_p)_s/\,(\rho C_p)_f \end{gathered}$$

Here prime represents the differentiation with respect to the similarity variable η. The appropriate boundary conditions are then given by:

$$\begin{gathered} f(c)=\frac{\varepsilon c}{2}+2\sigma c f''(c),\ \ f'(c)=\frac{\varepsilon}{2}+2\sigma f''(c),\\ \theta(c)=1,\\ f'(\eta)\to\frac{1-\varepsilon}{2},\ \ \theta(\eta)\to 0 \ \text{ as } \ \eta\to\infty, \end{gathered} \quad (10)$$

where $\varepsilon=U_w/U$ is the velocity ratio parameter between the needle and the free stream flow, $Pr=\nu/\alpha$ is the Prandtl number and $\sigma=ULr/\nu x$ is the slip parameter. It is worth knowing that the parameter σ is the function of x and its value varies locally throughout the flow motion.

The physical quantities of interest are the skin friction coefficients, C_f and the local Nusselt number, Nu_x which are defined as follows:

$$C_f = \frac{\mu_{nf}(\partial u/\partial r)_{r=c}}{\rho_f U^2}, \\ = \frac{4}{(1-\varphi)^{2.5}} Re_x^{-1/2} c^{1/2} f''(c), \qquad (11)$$

$$Nu_x = \frac{-xk_{nf}(\partial T/\partial r)_{r=c}}{k_f(T_w - T_\infty)}, \\ = -2\frac{k_{nf}}{k_f} Re_x^{1/2} c^{1/2} \theta'(0), \qquad (12)$$

where $Re_x = Ux/\nu$ is the local Reynolds number.

III. Stability Flow

In this study, a stability analysis is performed to know which of the solutions obtained are physically realistic or not. According to the previous studies by Weidman et al. (2006) and Rosca and Pop (2013), they found that the lower branch solutions are not physically realistic or said to be in unstable mode. Meanwhile, the opposite trend is noted for the upper branch solutions. To identify the stability of the solutions, we first consider the unsteady Equations (2) and (3) by introducing the new dimensionless time variable $\tau = 2Ut/x$. The function of τ is associated with an initial value problem that is consistent with the solution that will be obtained in practice (physically realistic).

Hence, the new similarity transformations in terms of η and τ for the Equation (6) are:

$$\psi = \nu x f(\eta,\tau),\ \theta(\eta,\tau) = \frac{T-T_\infty}{T_w - T_\infty},\ \eta = \frac{Ur^2}{\nu x}, \\ \tau = \frac{2Ut}{x}, \qquad (13)$$

Then, substituting Equation (13) into Equations (2) and (3) yields the following

$$\frac{2\eta}{A_1}\frac{\partial^3 f}{\partial \eta^3} + \frac{2}{A_1}\frac{\partial^2 f}{\partial \eta^2} + f\frac{\partial^2 f}{\partial \eta^2} - \frac{\partial^2 f}{\partial \eta \partial \tau} \\ + \tau\frac{\partial f}{\partial \eta}\frac{\partial^2 f}{\partial \eta \partial \tau} = 0, \qquad (14)$$

$$\frac{2\eta}{Pr}\frac{A_2}{A_3}\frac{\partial^2 \theta}{\partial \eta^2} + \frac{2}{Pr}\frac{A_2}{A_3}\frac{\partial \theta}{\partial \eta} + f\frac{\partial \theta}{\partial \eta} - \frac{\partial \theta}{\partial \tau} \\ + \tau\frac{\partial f}{\partial \eta}\frac{\partial \theta}{\partial \tau} = 0, \qquad (15)$$

along with the boundary conditions:

$$f(c,\tau) = \frac{\varepsilon c}{2} + 2\sigma c\frac{\partial^2 f}{\partial \eta^2}(c,\tau),\ \theta(c,\tau) = 1, \\ \frac{\partial f}{\partial \eta}(c,\tau) = \frac{\varepsilon}{2} + 2\sigma\frac{\partial^2 f}{\partial \eta^2}(c,\tau), \\ \frac{\partial f}{\partial \eta}(\eta,\tau) \to \frac{1-\varepsilon}{2},\ \theta(\eta,\tau) \to 0 \text{ as } \eta \to \infty, \qquad (16)$$

Afterwards, we assume (Rosca and Pop, 2013, Weidman et al., 2006)

$$f(\eta,\tau) = f_0(\eta) + e^{-\gamma\tau}F(\eta,\tau), \\ \theta(\eta,\tau) = \theta_0(\eta) + e^{-\gamma\tau}G(\eta,\tau), \qquad (17)$$

in order to identify the stability of the solution $f = f_0(\eta)$ and $\theta = \theta_0(\eta)$ satisfying the boundary value problem (14)–(16). Here, functions $F(\eta,\tau)$ and $G(\eta,\tau)$ are small relative to $f_0(\eta)$ and $\theta_0(\eta)$, respectively, and γ is an unknown eigenvalue parameter.

Substituting Equation (17) into Equations (14)–(16), we obtain the following linear eigenvalue problem:

$$\frac{2\eta}{A_1}F_0''' + \frac{2}{A_1}F_0'' + f_0F_0'' + f_0''F_0 + \gamma F_0' = 0, \qquad (18)$$

$$\frac{2\eta}{Pr}\frac{A_2}{A_3}G_0'' + \frac{2}{Pr}\frac{A_2}{A_3}G_0' + f_0G_0' + F_0\theta_0' \\ + \gamma G_0 = 0, \qquad (19)$$

subject to the boundary conditions

$$F_0(c) = 2\sigma c F_0''(c), F_0'(c) = 2\sigma F_0''(c), G_0(c) = 0, \\ F_0'(\eta) \to 0,\ G_0(\eta) \to 0,\ \text{as } \eta \to \infty. \qquad (20)$$

Note that, Harris et al. (2009) suggested that the range of possible eigenvalues can be determined by relaxing the boundary conditions on $F_0(\eta)$ or $G_0(\eta)$. In current study, we relax the condition $F_0(\eta) \to 0$ as $\eta \to \infty$ and then, solve the system of eigenvalue problem (18) and (19) subject to (20) together with the new condition $F_0''(c) = 1$. It should be note that, if the smallest eigenvalue γ is negative, the flow is unstable and there exists an initial growth of disturbances. In contrast to that, if the smallest eigenvalue γ is positive, the flow is stable and there is an initial decay of disturbances in the system.

IV. Numerical Approach

The bvp4c solver is one of the technique used to solve the boundary value problems that implemented in MATLAB software. This technique applies the finite difference method, where the solution can be obtained using an initial guess supplied at an initial mesh point and change step size to get the specified certainty. Nevertheless, to compute these boundary value problems, we must reduce it to a system of first order ordinary differential equations.

Now, we introduce the following variables

$$y_1 = f(\eta), \;\; y_2 = f'(\eta), \;\; y_3 = f''(\eta),$$
$$y_4 = \theta(\eta), \;\; y_5 = \theta'(\eta). \tag{21}$$

where

$$y_1' = y_2, \;\; y_2' = y_3, \;\; y_4' = y_5. \tag{22}$$

Thus, Equations (8) and (9) can be rewrite as

$$y_3' = -\frac{1}{\eta}\left[y_3 + \frac{A_1}{2} y_1 y_3\right] \tag{23}$$

$$y_5' = -\frac{1}{\eta}\left[y_5 + \frac{Pr}{2}\frac{A_3}{A_2} y_1 y_5\right] \tag{24}$$

with the transformed boundary conditions

$$ya_1 - \frac{\varepsilon c}{2} - 2\sigma c y a_3 = 0,$$
$$ya_2 - \frac{\varepsilon}{2} - 2\sigma y a_3 = 0, \;\; ya_4 - 1 = 0,$$
$$yb_2 - \frac{1-\varepsilon}{2} = 0, \;\; yb_4 = 0, \tag{25}$$

where a and b correspond to the conditions on the surface $\eta = 0$ and far field $\eta = \eta_\infty$, respectively. In this work, a suitable finite value of η_∞ is taken as $\eta = 60$ which depend on the values of the parameters used.

V. Results and Discussion

The ordinary differential equations (8) and (9) together with the conditions (10) are computed numerically using MATLAB bvp4c solver. The obtained results are presented for various values of the slip parameter σ, velocity ratio parameter ε, nanofluid volume fraction parameter ϕ when needle size $c = 0.1$ or $c = 0.2$ in some figures with the Prandtl number $Pr = 6.2$ (water). We let the range value of ϕ is between 0 (regular fluid) to 0.2. In addition, the thermophysical properties of solid nanoparticles and base fluid are given in the work of Oztop and Abu-Nada (2008).

Figures 1 and 2 illustrate the variations of the shear stress $f''(c)$ and local heat flux $-\theta'(c)$ with velocity ratio parameter ε for several values of slip parameter σ. It is noticed from the figures that as the slip parameter increases, the numerical value of shear stress and local heat flux also increases. This shows that the presence of the slip on the needle surface widens the range of the possible solutions exist. However, an increase in the slip parameter reduces the critical point by which the upper branch and lower branch solutions intersected. Note that, the dual solutions are likely to exist when the needle moves in the opposite way of the free stream flow $\varepsilon < 0$. It follows from Figures 1 and 2 that the dual solutions exist is in the range of $\varepsilon_c < \varepsilon \leq -0.5$. From these figures, the existence of unique solutions occurs for $\varepsilon > -0.5$.

Figures 3 and 4 present the effect of the needle sizes c on the variation of the shear stress and local heat flux with ε for Al_2O_3. As we can see, the values of $f''(c)$ and $-\theta'(c)$ is higher for the thinner surface compared to that of thicker

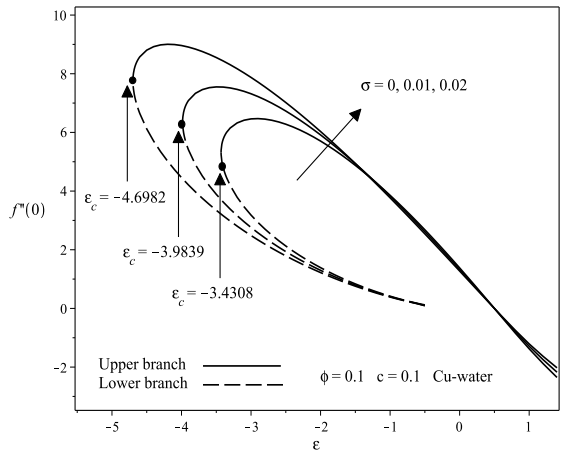

Figure 1: Effect of slip parameter σ on the variation of $f''(c)$ with velocity ratio parameter ε.

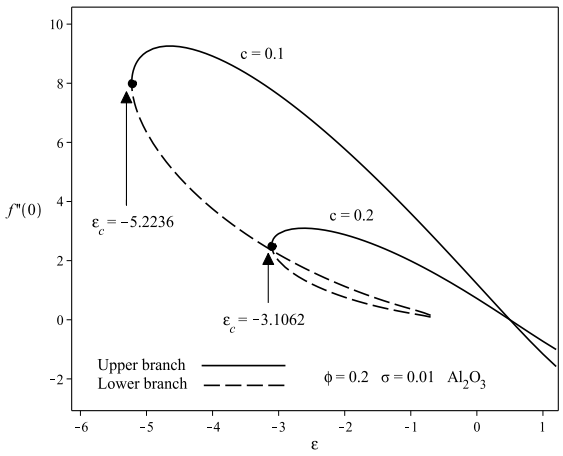

Figure 3: Effect of needle size c on the variation of $f''(c)$ with velocity ratio parameter ε.

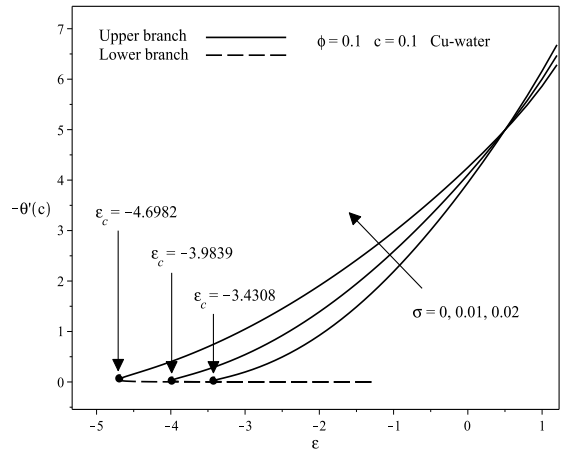

Figure 2: Effect of slip parameter σ on the variation of $-\theta'(c)$ with velocity ratio parameter ε.

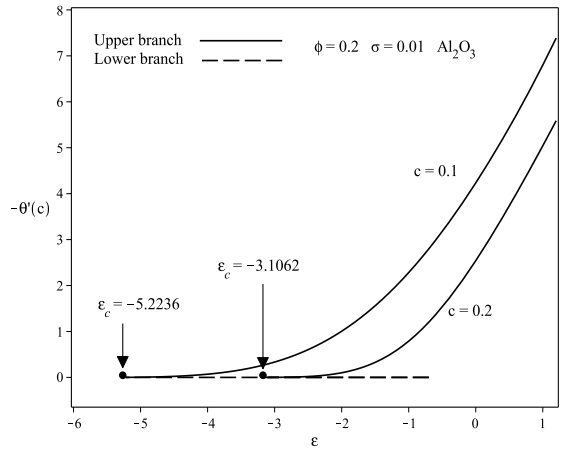

Figure 4: Effect of needle size c on the variation of $-\theta'(c)$ with velocity ratio parameter ε.

surface. Observation from Figure 3 yields that the thinner surface of the needle decreases the drag force occurs between the needle and the fluid flow and consequently, increases the shear stress on the surface. Interestingly, it is seen from Figure 4 that the process of heat transfer takes place quickly for $c = 0.1$. From the perspective of physics, thin surfaces allow heat to diffuse quickly through it. Besides, the graphs also shown that the range of the solutions obtained widens as the size of the needle decreases. However, the range of the dual solutions exist is between $\varepsilon_c < \varepsilon \leq -0.7$ for both values of $c = 0.1$ and $c = 0.2$.

The influence of the nanoparticles on the variation of the shear stress and local heat flux is illustrated in Figures 5 and 6 with velocity ratio parameter when $\sigma = 0.01$. It is noticed from the figures that range of the solutions exist is more pronounced for Al_2O_3 compared to others. Furthermore, the existence of the dual solutions for Equations (8) and (9) is observed in the range of $\varepsilon_c < \varepsilon \leq -0.7$. Within a certain range, say $-2.3 < \varepsilon \leq 0.5$, the magnitude of the shear stress and local heat flux on the needle surface is higher for Cu followed by

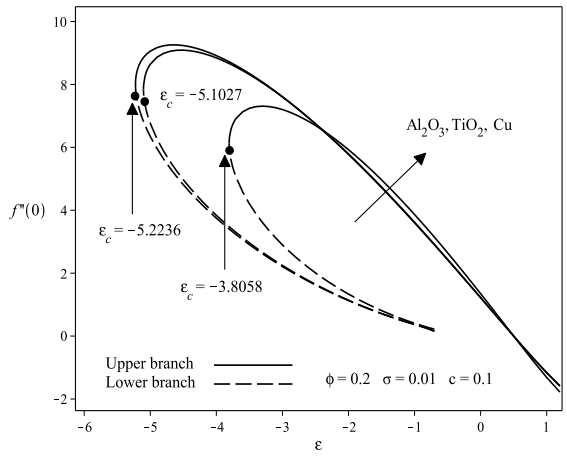

Figure 5: Effect of nanoparticles on the variation of $f''(c)$ with velocity ratio parameter ε.

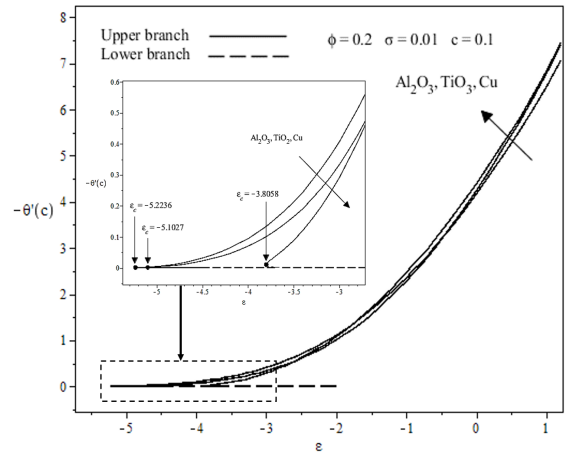

Figure 6: Effect of nanoparticles on the variation of $-\theta'(c)$ with velocity ratio parameter ε.

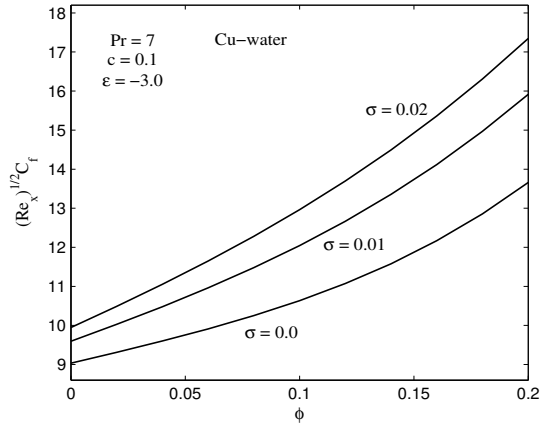

Figure 7: Effect of slip parameter σ on the variation of skin friction coefficients with nanoparticle volume fraction ϕ.

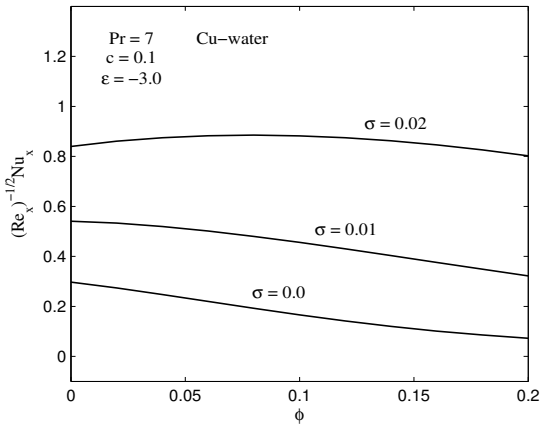

Figure 8: Effect of slip parameter σ on the variation of local Nusselt number with nanoparticle volume fraction ϕ.

TiO_2 and Al_2O_3. It follows Oztop and Abu-Nada (2008) that the highest heat transfer is obtained for Cu due to the higher thermal conductivity compared to TiO_2 and Al_2O_3.

Figures 7 and 8 depict the numerical values of the skin friction coefficient $(Re_x)^{1/2}C_f$ and local Nusselt number $(Re_x)^{-1/2}Nu_x$ with nanoparticle volume fraction ϕ for several values of slip parameter. The graphs yields that the skin friction coefficient and the heat transfer rate on the needle surface increases, as the slip parameter increase. This flow pattern implies that an increment in the slip parameter causes the momentum and thermal boundary layer to decrease. As a consequence, increases the shear stress and local heat flux, as well as the skin friction coefficients and heat transfer rate on the surface. Furthermore, the higher rate of a nanoparticle volume fraction leads to an increase in the skin friction coefficient as presented in Figure 7. Physically, the presence of nanofluid in the flow allows the nanoparticles and base fluid particles collide with each other, and this will enhance the friction occurring on the needle surface. As can be seen in

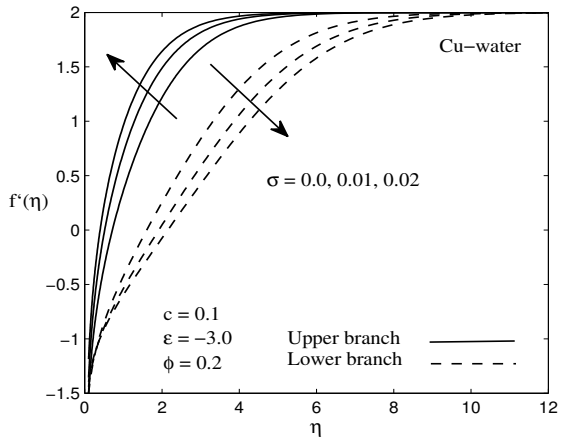

Figure 9: Effect of slip parameter σ on the variation of velocity profiles.

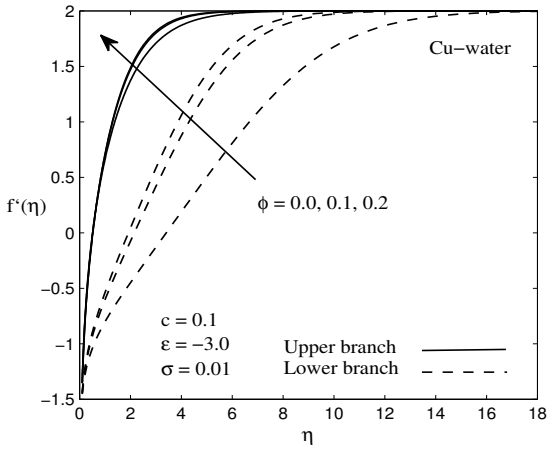

Figure 11: Effect of nanoparticle volume fraction ϕ on the variation of velocity profiles.

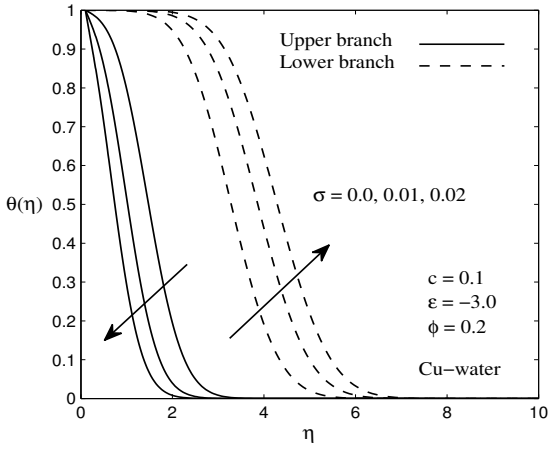

Figure 10: Effect of slip parameter σ on the variation of temperature profiles.

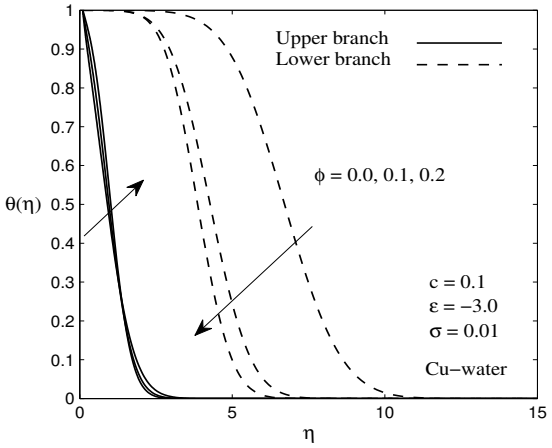

Figure 12: Effect of nanoparticle volume fraction ϕ on the variation of temperature profiles.

Figure 8, the rate of heat transfer decreases as the size of the nanoparticle increase. To prove this statement, we can look at Figure 12 where the temperature gradient increases, as the ϕ increase. It follows that the higher temperature gradients reduce the heat transfer rate occurs between the surface and the fluid flow.

Figures 9–12 depict the influence of the slip parameter and nanoparticle volume fraction parameter on the sample velocity and temperature profiles. It is noticed that the momentum and thermal boundary layer thickness for the lower branch solution is always thicker than the upper branch solution. It is worth knowing that, all the profiles obtained in Figures 9–12 has qualified the boundary conditions (10) asymptotically. Note that, the dual velocity and temperature profiles obtained in these figures also supported the existence of the dual solutions gained for Figures 1–6.

Furthermore, the determination of the stable solutions has been done using a stability analysis. The purpose of this analysis is to verify which of the upper or lower branch solution is linearly stable and physically realistic. This analysis is performed by substituting Equations

Table 1: Smallest eigenvalues γ for some values of slip parameter σ and velocity ratio parameter ε when $\phi = c = 0.1$ for Cu-water nanofluid.

σ	ε	Upper branch	Lower branch
0	-3.4306	0.0288	-0.0084
	-3.4304	0.0369	-0.0163
	-3.4302	0.0434	-0.0226
	-3.4300	0.0465	-0.0256
0.01	-3.9518	0.5701	-0.0040
	-3.9502	0.5777	-0.0104
	-3.9498	0.5794	-0.0120
	-3.9452	0.5999	-0.0294

(18) and (19) along with the conditions (20) into the bvp4c function in MATLAB software. The stability of the solutions depends on the sign of the eigenvalues γ obtained. Table 1 displays the smallest eigenvalue γ for different values of σ and ε. The table clearly indicates that the negative value of γ represents an initial growth of disturbance and the flow is unstable. In the meantime, the positive value of γ represents an initial decay of disturbance and the flow is stable. It should be noted that, the stable solution offers a good physical meaning which can be realized.

VI. Conclusion

In this work, the effects of partial slip on the boundary layer flow and heat transfer of a nanofluid past a thin needle moving in a parallel stream is analyzed. The reduced set of nonlinear ordinary differential equations is computed numerically using bvp4c function in MATLAB. The stability analysis is considered to find the stable solution. The results of the current study can be concluded as follows:

- The existence of the dual solutions is found to exist when the needle moves in the opposite way of free stream direction $\varepsilon < 0$, meanwhile the solution is unique when they move in the same way $\varepsilon > 0$.
- An increment in the slip parameter and the reduction of the needle size has widened the range of the solutions exist.
- The stability analysis has confirmed that the upper branch solution is stable solution, while the lower branch solution is unstable solution.
- Increases the slip and nanoparticle volume fraction parameter causes the skin friction coefficients on the needle surface to increase. Meanwhile, the opposite trend is observed for higher values of needle size.
- An increment in the needle size and the nanoparticle volume fraction leads to decrease the rate of heat transfer occur on the surface, while the opposite effect notes for higher values of slip parameter.
- Cu has a higher magnitude of the local heat flux in a certain range, say $-2.3 < \epsilon \leq 0.5$ because it has higher value of thermal conductivity compared to TiO_2 and Al_2O_3.

Overall, the presence of the slip effect in this work has contributed to an increment of heat transfer rate between the needle and the free stream flow due to the slip length. This increment of heat transfer is appropriate for some applications that required high heat transfer rate especially in the cooling process.

Acknowledgements

The authors wish to convey their genuine thanks to the referees for their essential comments and suggestions to progress the superiority of this manuscript. This work was supported by the Fundamental Research Grant Scheme (FRGS/1/2018/STG06/UPM/02/4/5540155), Ministry of Higher Education, Malaysia and Putra Grant GP-IPS/2018/9667900 from Universiti Putra Malaysia.

References

[1] M. I. Afridi and M. Qasim. Entropy generation and heat transfer in boundary layer flow over a thin needle moving in a parallel stream in the presence of nonlinear rosseland radiation. *Int. J. Therm. Sci.*, 123:117–128, 2018.

[2] S. Ahmad, N. M. Arifin, R. Nazar, and I. Pop. Mixed convection boundary layer flow along vertical thin needles: Assisting and opposing flows. *Int. Commun. Heat Mass Trans.*, 35:157–162, 2008.

[3] M. Awais, T. Hayat, A. Ali, and S. Irum. Velocity, thermal and concentration slip effects on a magneto-hydrodynamic nanofluid flow. *Alexandria Eng. J.*, 55:2107–2114, 2016.

[4] N. Bachok, A. Ishak, and I. Pop. Flow and heat transfer characteristics on a moving plate in nanofluid. *Int. J. Heat Mass Trans.*, 55:642–648, 2012.

[5] N. Bachok, A. Ishak, and I. Pop. Unsteady boundary-layer flow and heat transfer of a nanofluid over a permeable stretching/shrinking sheet. *Int. J. Heat Mass Trans.*, 55:2102–2109, 2012.

[6] G. S. Beavers and D. D. Joseph. Boundary condition at a naturally permeable wall. *J. Fluid Mech.*, 30:197–207, 1967.

[7] K. Bhattacharyya, G. C. Layek, and R. S. R. Gorla. Slip effect on boundary layer flow on a moving flat plate in a parallel free stream. *Int. J. Fluid Mech. Res.*, 39:438–447, 2012.

[8] J. Buongiorno. Convective transport in nanofluids. *J. Heat Trans.*, 128:240–250, 2006.

[9] S. U. S. Choi. Enhancing thermal conductivity of fluids with nanoparticles. *American Soc. Mech. Eng. Fluids Eng. Div.*, 231:99–105, 1995.

[10] K. Das. Slip effects on mhd mixed convection stagnation point flow of a micropolar fluid towards a shrinking vertical sheet. *Comp. Math. Appl.*, 63:255–267, 2012.

[11] T. Grosan and I. Pop. Forced convection boundary layer flow past nonisothermal thin needles in nanofluids. *J. Heat Trans.*, 133, 2011.

[12] S. D. Harris, D. B. Ingham, and I. Pop. Mixed convection boundary-layer flow near the stagnation point on a vertical surface in a porous medium: Brinkman model with slip. *Transp. Porous Media*, 77:267–285, 2009.

[13] T. Hayat, M. I. Khan, M. Farooq, T. Yasmeen, and A. Alsaedi. Water-carbon nanofluid flow with variable heat flux by a thin needle. *J. Mol. Liq.*, 224:786–791, 2016.

[14] G. Huminic and A. Huminic. Application of nanofluids in heat exchangers: A review. *Renew. Sustain. Energy Rev.*, 16: 5625–5638, 2012.

[15] A. Ishak, R. Nazar, and I. Pop. Boundary layer flow over a continuously moving thin needle in a parallel free stream. *Chin. Phys. Lett.*, 24:2895–2897, 2007.

[16] P. M. Krishna, R. P. Sharma, and N. Sandeep. Boundary layer analysis of persistent moving horizontal needle in blasius and sakiadis magnetohydrodynamic radiative nanofluid flows. *Nucl. Eng. Technol.*, 49:1654–1659, 2017.

[17] L. L. Lee. Boundary layer over a thin needles. *Phys. Fluids*, 10:1820–1822, 1967.

[18] T. R. Mahapatra and S. K. Nandy. Stability analysis of dual solutions in stagnation-point flow and heat transfer over a power-law shrinking surface. *Int. J. Nonlinear Sci.*, 12:86–94, 2011.

[19] J. P. Narain and S. M. Uberoi. Combined forced and free-convection heat transfer from vertical thin needles in a uniform stream. *Phys. Fluids*, 15:1879–1882, 1972.

[20] J. P. Narain and S. M. Uberoi. Combined forced and free-convection over thin needles. *Int. J. Heat Mass Trans.*, 16:1505–1512, 1973.

[21] N. A. Othman, N. A. Yacob, N. Bachok, A. Ishak, and I. Pop. Mixed convection boundary-layer stagnation point flow past a vertical stretching/shrinking surface in a nanofluid. *Appl. Therm. Eng.*, 115:1412–1417, 2017.

[22] H. F. Oztop and E. Abu-Nada. Numerical study of natural convection in partially heated rectangular enclosures filled with nanofluids. *Int. J. Heat Fluid Flow*, 29:1326–1336, 2008.

[23] A. K. Pandey and M. Kumar. Boundary layer flow and heat transfer analysis on cu-water nanofluid flow over a stretching cylinder with slip. *Alexandria Eng. J.*, 56:671–677, 2017.

[24] A. V. Rosca and I. Pop. Flow and heat transfer over a vertical permeable stretching/ shrinking sheet with a second order slip. *Int. J. Heat Mass Trans.*, 60: 355–364, 2013.

[25] R. Saidur, K. Y. Leong, and H. A. Mohammad. A review on applications and challenges of nanofluids. *Renew. Sustain. Energy Rev.*, 15:1646–1668, 2011.

[26] R. Sharma, A. Ishak, and I. Pop. Stability analysis of magnetohydrodynamic stagnation-point flow toward a stretching/shrinking sheet. *Comp. Fluids*, 102: 94–98, 2014.

[27] S. K. Soid, A. Ishak, and I. Pop. Boundary layer flow past a continuously moving thin needle in a nanofluid. *Appl. Therm. Eng.*, 114:58–64, 2017.

[28] R. K. Tiwari and M. K. Das. Heat transfer augmentation in a two-sided lid-driven differentially heated square cavity utilizing nanofluids. *Int. J. Heat Mass Trans.*, 50:2002–2018, 2007.

[29] R. Trimbitas, T. Grosan, and I. Pop. Mixed convection boundary layer flow along vertical thin needles in nanofluids. *Int. J. Numer. Methods Heat Fluid Flow*, 24:579–594, 2014.

[30] M. J. Uddin, W. A. Khan, and A. I. M. Ismail. Melting and second order slip effect on convective flow of nanofluid past a radiating stretching/shrinking sheet. *Propulsion Power Research*, 7:60–71, 2018.

[31] C. Y. Wang. Mixed convection on a vertical needle with heated tip. *Phys. Fluids*, 2:622–625, 1990.

[32] C. Y. Wang. Boundary condition at a naturally permeable wall flow due to a stretching boundary with partial slip-an exact solution of the navier–stokes equations. *Chem. Eng. Sci.*, 57:3745–3747, 2002.

[33] P. D. Weidman, D. G. Kubitschek, and A. M. J. Davis. The effect of transpiration on self-similar boundary layer flow over moving surfaces. *Int. J. Eng. Sci.*, 44:730–737, 2006.

[34] K. V. Wong and O. D. Leon. Applications of nanofluids: Current and future. *Adv. Mech. Eng.*, 2010:519659, 2010.

[35] M. H. M. Yasin, A. Ishak, and I. Pop. Boundary layer flow and heat transfer past a permeable shrinking surface embedded in a porous medium with a second-order slip: A stability analysis. *Appl. Ther. Eng.*, 115:1407–1411, 2017.